# Evaluating Benign and Malignant Bone and Soft-Tissue Lesions with Technetium-99m-MIBI Scintigraphy

Junichi Taki, Hisashi Sumiya, Hiroyuki Tsuchiya, Katsuro Tomita, Akitaka Nonomura and Norihisa Tonami
*Departments of Nuclear Medicine and Orthopedics, Kanazawa University School of Medicine; Pathology Section, Kanazawa University Hospital, Kanazawa, Japan*

This study compares the ability of $^{201}$Tl and $^{99m}$Tc-MIBI to detect and assess tumor response to chemotherapy in malignant and benign bone and soft-tissue lesions. **Methods:** Forty-two patients with various bone and soft-tissue pathologies (29 malignant and 13 benign lesions) were studied with $^{201}$Tl and $^{99m}$Tc-MIBI. Planar $^{201}$Tl scintigraphy was performed 15 min after injection of 111 MBq of $^{201}$Tl. Within 1 wk of the $^{201}$Tl study, radionuclide angiography with 600–740 MBq of $^{99m}$Tc-MIBI was performed and planar imaging was done 15 min later. **Results:** In visual analysis, 31 of 42 patients showed similar uptake of both tracers, 8 showed more intense uptake of $^{99m}$Tc-MIBI than $^{201}$Tl and 3 showed more intense uptake of $^{201}$Tl than $^{99m}$Tc-MIBI. In quantitative analysis, similar $^{201}$Tl and $^{99m}$Tc-MIBI uptake ratios were obtained (1.96 ± 1.25 versus 1.96 ± 1.02, respectively; p = ns). The perfusion index derived from $^{99m}$Tc-MIBI radionuclide angiography was higher than $^{99m}$Tc-MIBI uptake ratio (2.33 ± 1.23 versus 1.96 ± 1.02, respectively; $p < 0.005$), but correlated well with $^{99m}$Tc-MIBI uptake ratio (r = 0.75). In 11 patients with malignant tumors, $^{201}$Tl and $^{99m}$Tc-MIBI scintigraphy was repeated after chemotherapy and the uptake of both tracers was significantly suppressed in patients with complete response confirmed by histological evaluation. In patients with complete response (n = 3), the uptake ratio of both tracers was reduced by more than 50%, whereas, less than 20% reduction of uptake ratio was observed in patients with nonresponse (n = 6). **Conclusion:** The ability of $^{99m}$Tc-MIBI to detect malignant and benign bone and soft-tissue lesions and to assess tumor response to chemotherapy was comparable to that of $^{201}$Tl. In addition, blood flow could be assessed by radionuclide angiography with $^{99m}$Tc-MIBI. Technetium-99m-MIBI is a promising radiopharmaceutical for the evaluation of bone and soft-tissue lesions.

**Key Words:** technetium-99m-MIBI; thallium-201; bone tumor; soft-tissue tumor; chemotherapy

**J Nucl Med 1997; 38:501–506**

Technetium-99m-hexakis-2-methoxyisobutylisonitrile (MIBI) was developed as a myocardial perfusion imaging agent. It has also been widely used as a tumor imaging agent in various benign and malignant lesions, including lung, breast, thyroid and brain tumors and lymphoma (*1–6*), because it accumulates in viable tumor cells through the potassium pathway with the ATPase-dependent $Na^+/K_+$ pump (*7*). Recently, $^{99m}$Tc-MIBI also has been used in the detection of various benign and malignant tumors (*8–15*).

In bone and soft-tissue tumors, $^{201}$Tl and $^{99m}$Tc-MIBI scintigraphy was proven to be a valuable diagnostic method (*16,17*). However, no study has compared $^{201}$Tl and $^{99m}$Tc-MIBI in such tumors. Since $^{99m}$Tc-MIBI is labeled with $^{99m}$Tc, it is not only more appropriate for imaging than $^{201}$Tl but also, since a higher dose can be used, tumor perfusion can be evaluated simultaneously by radionuclide angiography. Furthermore, $^{99m}$Tc-MIBI is practical in routine practice because of its continuous availability as a kit-based agent. In this study, $^{201}$Tl and $^{99m}$Tc-MIBI accumulation and response to chemotherapy, in the same patients with bone and soft-tissue lesions, were evaluated and lesion perfusion by radionuclide angiography with $^{99m}$Tc-MIBI was assessed.

## MATERIALS AND METHODS

### Patients

The study comprised 42 patients with various bone and soft-tissue disorders proven pathologically in specimens obtained by biopsy and/or surgery. There were 21 men and 21 women (age range 8–87 yr; average age 47 ± 21 yr). Twenty-nine had malignant tumors (3 osteosarcomas, 1 parosteal osteosarcoma, 4 chondrosarcomas, 6 malignant fibrous histiocytomas, 1 epitheloid sarcoma, 1 synovial cell sarcoma, 3 malignant schwannomas, 1 myxoid liposarcoma, 1 multiple myeloma, 1 non-Hodgkin's lymphoma, 7 bone metastatic adenocarcinoma) and 13 had benign lesions (1 giant-cell tumor, 2 neurinomas, 2 neurilemmomas, 2 bone cysts (1 with traumatic fracture), 1 enchondroma, 2 abscesses, 1 osteomyelitis, 1 nonspecific lymph node swelling, 1 postchemotherapeutic nonspecific fibrous tissue).

### Thallium-201 and Technetium-99m-MIBI Imaging

Planar 3-min $^{201}$Tl imaging was performed 15 min after intravenous injection of 111 MBq of the radiopharmaceutical with a gamma camera equipped with a low-energy, high-resolution, parallel-hole collimator.

Within 1 wk of the $^{201}$Tl study, radionuclide angiography was performed after injection of 600–740 MBq $^{99m}$Tc-MIBI with a gamma camera equipped with a low-energy, high-resolution, parallel-hole collimator. Data were acquired every 2 sec for 2 min. Then, planar 3-min $^{99m}$Tc-MIBI images were obtained 15 min after radionuclide administration.

### Image Analysis

Both $^{201}$Tl and $^{99m}$Tc-MIBI images were evaluated visually and quantitatively. For visual analysis, two blinded observers evaluated the degree of radionuclide uptake using a five-grade scoring system, with 0 = background activity, 1+ = slight increase in uptake, 2+ = moderate uptake, 3+ = strong uptake but less than heart, 4+ = strong uptake equal to or greater than heart. Radionuclide angiography with $^{99m}$Tc-MIBI was also evaluated by two blinded observers and the degree of perfusion increase was classified into four grades, with 0 = no increase, 1+ = mild increase, 2+ = moderate increase, 3+ = marked increase in arterial phase.

Received Nov. 22, 1995; revision accepted May 8, 1996.

For correspondence or reprints contact: Junichi Taki, MD, Department of Nuclear Medicine, Kanazawa University School of Medicine, 13-1 Takara-machi, Kanazawa, 920 Japan.

**TABLE 1**
Scintigraphic Findings with Technetium-99m-MIBI and Thallium-201 in All Patients

| Patient no. | Age (yr) | Sex | Diagnosis (tumor grade) | Lesion site | $^{99m}$Tc-MIBI Visual perfusion | $^{99m}$Tc-MIBI Perfusion index | $^{99m}$Tc-MIBI Visual uptake | $^{99m}$Tc-MIBI Uptake ratio | $^{201}$Tl Visual uptake | $^{201}$Tl Uptake ratio |
|---|---|---|---|---|---|---|---|---|---|---|
| Malignant lesions | | | | | | | | | | |
| 1 | 16 | M | Osteosarcoma (high) | Right humerus | 2 | 2.46 | 2 | 1.63 | 2 | 1.48 |
| 2 | 8 | M | Osteosarcoma (high) | Right humerus | 2 | 1.99 | 2 | 1.76 | 2 | 2.41 |
| 3 | 21 | M | Osteosarcoma (high) | Right femur | 3 | 3.33 | 3 | 2.12 | 3 | 2.10 |
| 4 | 34 | F | Parosteal osteosarcoma (low) | Right femur | 2 | 1.95 | 2 | 1.40 | 2 | 1.43 |
| 5 | 73 | F | Chondrosarcoma (high) | Left femur | 3 | 3.23 | 1 | 1.18 | 1 | 1.20 |
| 6 | 32 | F | Chondrosarcoma (low) | Left femur | 0 | 1.01 | 0 | 0.86 | 0 | 1.12 |
| 7 | 81 | M | Chondrosarcoma (low) | Right thumb | 2 | 2.42 | 2 | 3.83 | 2 | 3.18 |
| 8 | 28 | M | Chondrosarcoma (low) | Right pelvis | 1 | 1.55 | 0 | 1.07 | 0 | 1.25 |
| 9 | 64 | M | Malignant fibrous histiocytoma (high) | Right pelvis | 2 | 2.84 | 2 | 1.79 | 3 | 2.41 |
| 10 | 39 | M | Malignant fibrous histiocytoma (high) | Lumbar subcutaneum | 1 | 1.83 | 2 | 1.43 | 0 | 1.21 |
| 11 | 69 | M | Malignant fibrous histiocytoma (high) | Right thigh | 1 | 1.55 | 2 | 1.55 | 1 | 1.54 |
| 12 | 66 | F | Malignant fibrous histiocytoma (high) | Left buttock | 2 | 3.53 | 2 | 1.78 | 1 | 1.54 |
| 13 | 67 | F | Malignant fibrous histiocytoma (high) | Right femur | 3 | 3.58 | 3 | 3.84 | 3 | 4.89 |
| 14 | 58 | F | Malignant fibrous histiocytoma (high) | Right upper arm | 0 | 0.95 | 0 | 1.17 | 0 | 0.97 |
| 15 | 58 | M | Epitheloid sarcoma (high) | Right thigh | 3 | 4.21 | 3 | 2.41 | 3 | 1.47 |
| 16 | 35 | F | Synovial cell sarcoma (high) | Left plantar | 2 | 2.50 | 2 | 3.30 | 2 | 3.00 |
| 17 | 18 | M | Malignant schwannoma (low) | Left retroperitoneum | 0 | 1.12 | 0 | 1.13 | 0 | 1.03 |
| 18 | 40 | M | Malignant schwannoma (high) | Right neck | 0 | 1.00 | 0 | 1.34 | 1 | 1.58 |
| 19 | 23 | F | Malignant schwannoma (high) | Right axilla | 0 | 1.18 | 3 | 1.68 | 2 | 1.51 |
| 20 | 53 | M | Myxoid liposarcoma (high) | Right thigh | 0 | 1.05 | 0 | 1.13 | 0 | 0.97 |
| 21 | 62 | M | Multiple myeloma | Sacrum | 2 | 2.68 | 2 | 2.31 | 1 | 1.72 |
| 22 | 49 | M | Metastatic adenocarcinoma | Left femur | 3 | 4.92 | 3 | 3.77 | 3 | 5.56 |
| 23 | 67 | M | Metastatic adenocarcinoma | Right pelvic bone | 3 | 2.94 | 2 | 1.50 | 3 | 1.53 |
| 24 | 70 | F | Metastatic adenocarcinoma | Left pelvic bone | 2 | 2.04 | 2 | 2.24 | 2 | 1.79 |
| 25 | 61 | F | Metastatic adenocarcinoma | Left femur | 3 | 4.06 | 3 | 4.74 | 3 | 6.16 |
| 26 | 51 | F | Metastatic adenocarcinoma | Thoracic vertebra (6–8) | 0 | 1.03 | 0 | 1.05 | 0 | 0.98 |
| 27 | 73 | M | Metastatic adenocarcinoma | Right radius | 3 | 3.88 | 2 | 2.39 | 2 | 2.26 |
| 28 | 87 | M | Metastatic adenocarcinoma | Left forearm | 1 | 1.28 | 2 | 2.17 | 2 | 1.79 |
| 29 | 72 | F | Non-Hodgkin's lymphoma | Left buttock | 2 | 2.19 | 3 | 1.85 | 2 | 2.59 |
| Benign lesions | | | | | | | | | | |
| 30 | 29 | F | Giant cell tumor | Right femur | 3 | 6.32 | 3 | 4.50 | 3 | 4.68 |
| 31 | 48 | M | Neurinoma | Right calf | 2 | 2.50 | 2 | 1.63 | 1 | 1.64 |
| 32 | 73 | M | Neurinoma | Left thigh | 1 | 1.29 | 0 | 1.06 | 0 | 0.96 |
| 33 | 28 | F | Neurilemmoma | Left iliac | 0 | 1.01 | 0 | 0.95 | 0 | 0.87 |
| 34 | 71 | F | Neurilemmoma | Sacrum | 2 | 3.08 | 2 | 3.83 | 2 | 2.49 |
| 35 | 23 | F | Bone cyst with fracture | Left humerus | 1 | 1.96 | 1 | 1.54 | 1 | 0.93 |
| 36 | 21 | F | Bone cyst | Right femur | 0 | 1.52 | 0 | 1.22 | 0 | 1.03 |
| 37 | 34 | F | Enchondroma | Left humerus | 0 | 1.00 | 0 | 0.99 | 0 | 1.21 |
| 38 | 23 | F | Abscess (chronic) | Right thigh | 2 | 3.18 | 2 | 2.31 | 1 | 1.50 |
| 39 | 24 | F | Abscess (chronic) | Right poplitea | 3 | 3.15 | 2 | 1.74 | 2 | 1.75 |
| 40 | 20 | M | Osteomyelitis (chronic) | Left femur | 2 | 2.45 | 2 | 1.50 | 2 | 1.87 |
| 41 | 41 | F | Nonspecific lymph node swelling | Right elbow | 0 | 1.14 | 1 | 1.45 | 1 | 1.54 |
| 42 | 47 | M | Nonspecific fibrous tissue | Left calf | 0 | 1.01 | 0 | 0.99 | 0 | 1.01 |

For quantitative analysis, a manual ROI was set on the lesion and a symmetrical ROI was set on the contralateral normal area. Then, the uptake ratio was calculated by dividing the count density of the lesion by that of the contralateral normal area. In one patient with malignant fibrous histiocytoma adjacent to the spinal process and in a patient with vertebral metastasis, the reference ROI was set on the caudal side of the lesion.

The perfusion index was obtained by radionuclide angiography. Using the same ROI set to calculate the uptake ratio, the time-activity curve of each ROI was generated and the perfusion index was determined by dividing the peak count of the arterial phase of the lesion by that of the contralateral normal side. When a peak count was not obtained, the time-activity curve always showed a shoulder point, which was the flection point between the rapid count increase due to arterial phase and steady state or gradual count increase due to $^{99m}$Tc-MIBI accumulation to the lesion and normal tissue. Therefore, the count of the flexion point of the time-activity curve was used to calculate the perfusion index.

### Evaluation of Chemotherapy

Eleven patients with malignant tumors (3 osteosarcomas, 4 malignant fibrous histiocytomas, 1 malignant schwannoma, 2 bone metastasis (adenocarcinoma), 1 synovial cell sarcoma) underwent both pre- and postchemotherapy evaluation on both $^{99m}$Tc-MIBI and $^{201}$Tl imaging. Postoperative histological assessment was performed on these 11 patients to evaluate tumor response to chemotherapy. Histologic grading of the effect of chemotherapy was based on the degree of cellularity and necrosis in the largest slice of the resected tumor. Grade IV (100% necrosis) was considered a complete response and Grade III (>90% ~<100% necrosis) was considered a partial response. Grade II and I

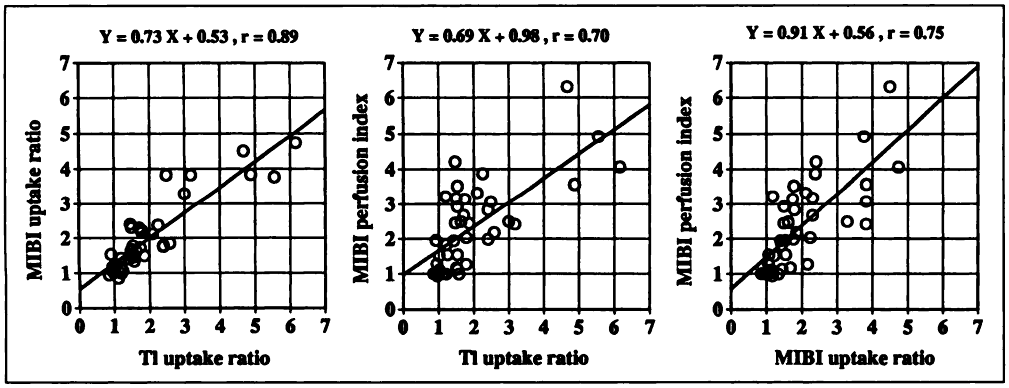


**FIGURE 1.** Correlations between $^{201}$Tl and $^{99m}$Tc-MIBI uptake ratio, $^{201}$Tl uptake ratio and $^{99m}$Tc-MIBI perfusion index, and $^{99m}$Tc-MIBI uptake ratio and $^{99m}$Tc-MIBI perfusion index. There is good correlation between $^{201}$Tl and $^{99m}$Tc-MIBI uptake ratios, while there are fair correlations between $^{201}$Tl uptake ratio and $^{99m}$Tc-MIBI perfusion index and between $^{99m}$Tc-MIBI uptake ratio and $^{99m}$Tc-MIBI perfusion index.

responses (≤90% ~>50% and ≤50%, respectively) were considered nonresponses.

To evaluate the effect of chemotherapy, percent changes in the perfusion index and uptake ratio (Δ%) were calculated by the following formula:

$$\Delta\% = 100 \times (\text{post-pre})/\text{pre},$$

where post = postchemotherapy value of perfusion index or uptake ratio and pre = prechemotherapy value of the perfusion index or uptake ratio.

### Statistical Analysis

Values are presented as mean ± s.d. Statistical comparisons were done using a two-tailed paired Student's t-test to compare the $^{201}$Tl and $^{99m}$Tc-MIBI uptake ratios and the $^{99m}$Tc-MIBI perfusion index. For comparisons of the perfusion index and uptake ratios between malignant and benign lesions and between low-grade and high-grade malignant lesions, a two-tailed unpaired Student's t-test was used. Comparison of proportion was performed with chi-square analysis. A p value of < 0.05 was considered significant.

## RESULTS

Patient data are summarized in Table 1 for malignant and benign lesions, respectively. Visual analysis of 31 of 42 patients showed similar uptake for both tracers, 8 (6 malignant and 2 benign lesions) showed more intense uptake of $^{99m}$Tc-MIBI than $^{201}$Tl and 3 (all malignant lesions) showed more intense uptake of $^{201}$Tl than $^{99m}$Tc-MIBI. In a patient with osteosarcoma (Patient 2), bone marrow extension was detected only with $^{99m}$Tc-MIBI. A malignant fibrous histiocytoma in Patient 10 was detected by $^{99m}$Tc-MIBI only, while a malignant schwannoma in Patient 18 was detected by $^{201}$Tl only. In 29 malignant lesions, 6 lesions (2 chondrosarcoma, 1 malignant fibrous histiocytoma, 1 myxoid liposarcoma, 1 malignant schwannoma, 1 vertebral bone metastatic adenocarcinoma) were not visualized on either $^{99m}$Tc-MIBI or $^{201}$Tl images. In benign lesions, all inflammatory lesions (2 abscesses, 1 osteomyelitis) and a giant-cell tumor showed intense uptake on both $^{99m}$Tc-MIBI and $^{201}$Tl images. A chondrosarcoma and a neurinoma in one patient each were detected only with radionuclide angiography.

Technetium-99m-MIBI background activity around the lesion was visually higher than $^{201}$Tl in 17 patients, equal to $^{201}$Tl in 19 patients and lower than $^{201}$Tl in 6 patients. In lung uptake of both tracers, each pattern was observed in 22, 17 and 3 patients, respectively.

In all patients, uptake ratios of $^{99m}$Tc-MIBI and $^{201}$Tl were similar (1.96 ± 1.02 versus 1.96 ± 1.25; p=ns). Uptake ratios of $^{99m}$Tc-MIBI in malignant and benign lesions were 2.01 ± 0.99 and 1.82 ± 1.11, respectively, and were similar to those of $^{201}$Tl (2.09 ± 1.34 and 1.65 ± 1.02, respectively; p=ns). In all patients, the perfusion index derived from dynamic $^{99m}$Tc-MIBI study was 2.33 ± 1.23 and was significantly higher than that of the $^{99m}$Tc-MIBI uptake ratio (1.96 ±1 .02; $p < 0.005$) and $^{201}$Tl uptake ratio (1.96 ± 1.25; $p < 0.05$). In malignant lesions, the $^{99m}$Tc-MIBI perfusion index (2.36 ± 1.13) was higher than the $^{99m}$Tc-MIBI uptake ratio (2.01 ± 0.99; $p < 0.05$) and $^{201}$Tl uptake ratio (2.09 ± 1.34; $p = 0.19$) but the difference was not significant between $^{99m}$Tc-MIBI perfusion index and $^{201}$Tl. In benign lesions, the $^{99m}$Tc-MIBI perfusion index (2.28 ± 1.48) was significantly higher than the $^{99m}$Tc-MIBI uptake ratio (1.82 ± 1.11; $p < 0.05$) and $^{201}$Tl uptake ratio (1.65 ± 1.02; $p < 0.01$). Good correlation was obtained between the $^{201}$Tl and $^{99m}$Tc-MIBI uptake ratios ($r = 0.89$), and fair ones were obtained between $^{201}$Tl uptake ratio and $^{99m}$Tc-MIBI perfusion index ($r = 0.70$) and between the $^{99m}$Tc-MIBI uptake ratio and perfusion index ($r = 0.75$) (Fig. 1).

Malignant lesions were not differentiated from benign lesion in both tracers (in malignant and benign lesions, respectively: perfusion index: 2.36 ± 1.13 versus 2.28 ± 1.48; $^{99m}$Tc-MIBI uptake ratio: 2.01 ± 0.99 versus 1.82 ± 1.11; $^{201}$Tl uptake ratio: 2.09 ± 1.34 versus 1.65±1.02). In 20 primary malignant lesions, both tracers did not accumulate in three of five low-grade tumors but did not accumulate in only three of 15 high-grade tumors, however, this was not significant (p = 0.01). There were no significant differences between low-grade and high-grade tumors in the perfusion index (1.61 ± 0.59 versus 2.35 ± 1.08), the $^{99m}$Tc-MIBI uptake ratio (1.66 ± 1.23 versus 1.87 ± 0.78) and the $^{201}$Tl uptake ratio (1.60 ± 0.90 versus 1.86 ± 1.01).

Changes in the perfusion index and uptake ratios of $^{99m}$Tc-MIBI and $^{201}$Tl before and after chemotherapy are shown in Table 2. In all patients with a pathological complete response, the perfusion index and uptake ratio of both tracers decreased significantly to 1.2 or less after chemotherapy. On the other hand, in patients with pathological nonresponse, neither the perfusion index nor uptake ratio decreased to 1.2 or less. As shown in Figure 2, good correlation was observed between the percent change in $^{99m}$Tc-MIBI and $^{201}$Tl uptake ratios as well as fair correlation between the percent change in the $^{99m}$Tc-MIBI perfusion index in $^{201}$Tl uptake ratio ($r = 0.83$ and $r = 0.69$, respectively). The percent change in the $^{99m}$Tc-MIBI uptake ratio and $^{99m}$Tc-MIBI perfusion index also showed good correlation ($r = 0.80$). In all three patients with complete response, the percent change in $^{99m}$Tc-MIBI and $^{201}$Tl uptake ratios was less than −50%. On the other hand, in all six patients with nonresponse, the percent change in both $^{99m}$Tc-MIBI and $^{201}$Tl uptake ratios was more than −20%.

Representative patients are shown in Figures 3, 4 and 5. Figure 3 compares the $^{201}$Tl and $^{99m}$Tc-MIBI images in a 67-yr-old woman with malignant fibrous histiocytoma of the

**TABLE 2**
Changes in the Perfusion Index and Uptake Ratios Before and After Chemotherapy on Technetium-99m-MIBI and Thallium-201 Images

| Patient no. | Diagnosis | $^{99m}$Tc-MIBI perfusion index Pre | Post | % change | $^{99m}$Tc-MIBI uptake ratio Pre | Post | % change | $^{201}$Tl uptake ratio Pre | Post | % change | Histologic response |
|---|---|---|---|---|---|---|---|---|---|---|---|
| 1 | Osteosarcoma | 2.46 | 2.09 | −15 | 1.63 | 1.27 | −22 | 1.48 | 1.15 | −22 | PR |
| 2 | Osteosarcoma | 1.99 | 1.12 | −44 | 1.76 | 0.78 | −56 | 2.41 | 1.01 | −58 | CR |
| 3 | Osteosarcoma | 3.33 | 1.00 | −70 | 2.12 | 1.02 | −52 | 2.10 | 0.95 | −55 | CR |
| 9 | Malignant fibrous histiocytoma | 2.84 | 5.35 | +88 | 1.79 | 2.31 | +29 | 2.41 | 2.71 | +12 | NR |
| 10 | Malignant fibrous histiocytoma | 1.83 | 1.73 | −5 | 1.43 | 1.36 | −5 | 1.21 | 1.46 | +21 | NR |
| 12 | Malignant fibrous histiocytoma | 3.53 | 1.93 | −45 | 1.78 | 1.44 | −19 | 1.54 | 1.56 | +1 | NR |
| 13 | Malignant fibrous histiocytoma | 3.58 | 1.82 | −49 | 3.84 | 2.87 | −25 | 4.89 | 1.66 | −66 | PR |
| 16 | Synovial cell sarcoma | 2.50 | 1.20 | −52 | 3.30 | 1.10 | −67 | 3.00 | 0.92 | −69 | CR |
| 19 | Malignant schwannoma | 1.18 | 1.26 | +7 | 1.68 | 1.64 | −2 | 1.51 | 1.39 | −8 | NR |
| 23 | Metastatic adenocarcinoma | 2.94 | 1.79 | −39 | 1.50 | 1.55 | +3 | 1.53 | 1.26 | −18 | NR |
| 25 | Metastatic adenocarcinoma | 4.06 | 4.65 | +15 | 4.74 | 5.30 | +12 | 6.16 | 5.96 | −3 | NR |

right distal femur. Radionuclide angiography revealed a hypervascular lesion. Both $^{201}$Tl and $^{99m}$Tc-MIBI demonstrated intense tracer uptake. The edge of the tumor was delineated slightly more sharply with $^{99m}$Tc-MIBI than with $^{201}$Tl.

Figure 4 shows an 8-yr-old boy with osteosarcoma in the right proximal humerus (Patient 2). Markedly increased tumor perfusion was demonstrated by radionuclide angiography with $^{99m}$Tc-MIBI. Although both $^{99m}$Tc-MIBI and $^{201}$Tl scintigraphy demonstrated increased uptake in the right proximal humerus, only $^{99m}$Tc-MIBI scintigraphy disclosed bone marrow extension to the humeral shaft. After chemotherapy, no significant increased tumor perfusion or $^{99m}$Tc-MIBI or $^{201}$Tl accumulation was observed. The surgical specimen revealed complete tumor necrosis.

Figure 5 shows a 72-yr-old woman with non-Hodgkin's lymphoma on the left buttock (Patient 29). Technetium-99m-MIBI showed stronger uptake than $^{201}$Tl, but the $^{99m}$Tc-MIBI uptake ratio was lower than $^{201}$Tl due to high background uptake.

## DISCUSSION

Generally, bone, $^{67}$Ga and $^{201}$Tl scintigraphy have been used to evaluate bone and soft-tissue lesions. Bone scintigraphy is quite sensitive for the detection of primary bone tumors as well as bone involvement by adjoining soft-tissue malignant tumors or metastasis. However, in defining the accurate extent of the tumor, $^{201}$Tl scintigraphy is more helpful than bone scintigraphy, even in the case of primary bone tumors. In addition, $^{201}$Tl scintigraphy is superior to bone scintigraphy and $^{67}$Ga imaging in predicting tumor response to chemotherapy (*16,17*).

Recently, $^{99m}$Tc-MIBI has been introduced as a myocardial perfusion imaging agent to replace $^{201}$Tl. Technetium-99m-MIBI has lipophilic cationic properties, accumulating largely in mitochondria by its negative transmembrane potential. Moreover, its accumulation depends on cell viability and metabolic conditions (*18–20*). In human carcinoma cell lines, mitochondria and plasma membrane potentials may also contribute to $^{99m}$Tc-MIBI uptake, and carcinoma cells accumulate $^{99m}$Tc-MIBI like myocardial cells (*21,22*). In addition, high-level expression of p-glycoprotein that is encoded by multidrug-resistance gene restricts $^{99m}$Tc-MIBI uptake in animal and human cell lines (*23–25*). Thallium-201 accumulation in a tumor largely depends on the sodium-potassium pump activity and, to some extent, tumor blood flow (*26,27*). Despite these suggested differences in uptake mechanisms, accumulation of $^{201}$Tl and $^{99m}$Tc-MIBI in various tumors was broadly similar to that reported in previous studies (*8–10*). Aktolun et al. (*8*) compared $^{99m}$Tc-MIBI and $^{201}$Tl uptake in 17 patients with malignant tumors, mainly lung and breast cancer, and found that both tracers accumulated in tumors except for one patient with breast cancer, in whom tumors were detected only by $^{99m}$Tc-MIBI. In six patients with brain tumors, O'Tuama et al. (*10*) showed that both $^{99m}$Tc-MIBI and $^{201}$Tl accumulated similarly, but the tumor-to-normal brain ratio was higher with $^{99m}$Tc-MIBI. In this study, 31 of 42 patients showed visually similar accumulation of both tracers, but eight showed greater $^{99m}$Tc-MIBI accumulation and three showed greater $^{201}$Tl uptake. The lesion-to-contralateral normal side uptake ratio of all patients was similar for $^{99m}$Tc-MIBI (1.96 ± 1.02) and $^{201}$Tl (1.96 ± 1.25), and for good correlation was observed between the uptake ratios of both tracers ($r = 0.89$), suggesting that similar factors were involved in the uptake of both tracers by lesions in spite of different cellular uptake mechanisms.

The uptake of both $^{99m}$Tc-MIBI and $^{201}$Tl tended to be higher in malignant lesions but not significantly so. In our experience

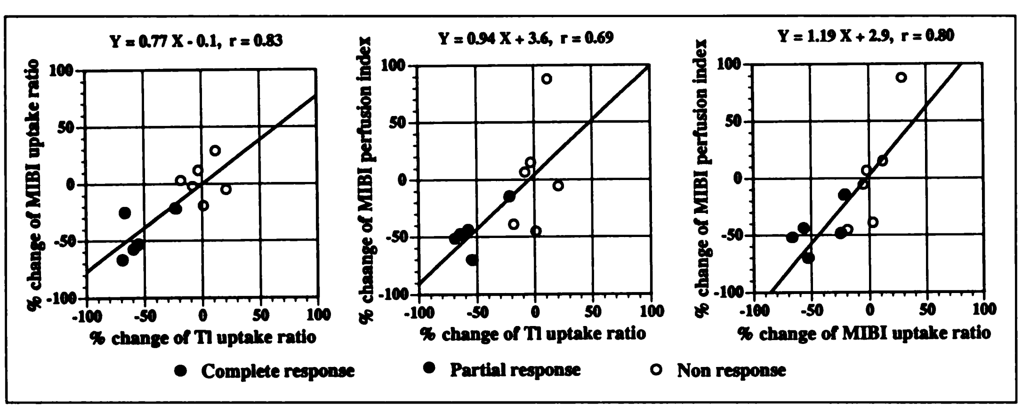


**FIGURE 2.** Changes in uptake ratio and perfusion index after chemotherapy. There are good correlations between percent changes in $^{201}$Tl and $^{99m}$Tc-MIBI uptake ratios and between $^{99m}$Tc-MIBI uptake ratio and perfusion index. There is fair correlation between percent changes in $^{201}$Tl uptake ratio and of $^{99m}$Tc-MIBI perfusion index.

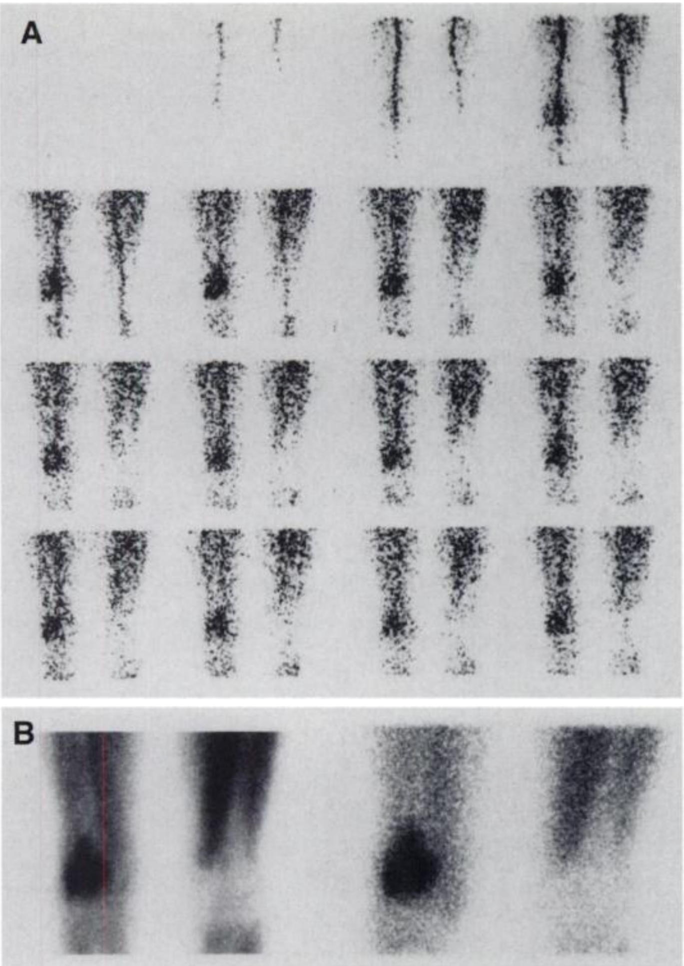


**FIGURE 3.** A 67-yr-old woman with malignant fibrous histicytoma in the right distal femur (Patient 13). (A) Radionuclide angiography with $^{99m}$Tc-MIBI shows markedly increased tumor perfusion in the right distal femur. (B) Both $^{99m}$Tc-MIBI (left) and $^{201}$Tl (right) scintigraphy show intense accumulation in the lesion. In this patient, muscle uptake was greater with $^{99m}$Tc-MIBI than $^{201}$Tl.

from this study and from our previous $^{201}$Tl study, we feel that the differentiation of malignant from benign lesions should be carefully judged because tracer uptake depends on several factors, including blood flow, proportion of viable parenchymal tumor cell component to stromal tissue and presence of tumor necrosis. For example, giant-cell tumors (n = 11) always

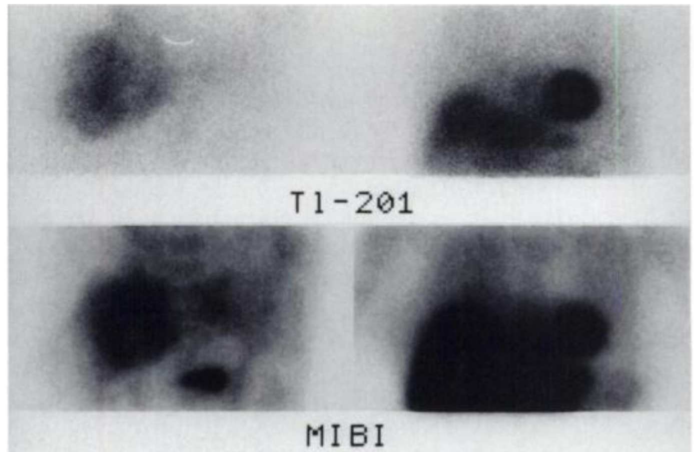


**FIGURE 5.** A 72-yr-old woman with non-Hodgkin's lymphoma on the left buttock (Patient 29). Images of both tracers were normalized with maximal myocardial counts of each tracer. Technetium-99m-MIBI posterior image shows stronger uptake than $^{201}$Tl, but the $^{99m}$Tc-MIBI uptake ratio (1.85) was lower than that for $^{201}$Tl (2.59) due to high background uptake.

showed intense $^{201}$Tl uptake (we have only one patient studied with $^{99m}$Tc-MIBI) and malignant schwannoma and chondrosarcoma usually showed poor or low $^{201}$Tl and $^{99m}$Tc-MIBI uptake.

Since $^{99m}$Tc-MIBI is a technetium-labeled radiopharmaceutical, administration of a sufficient dose for radionuclide angiography is possible. Therefore, tumor blood flow can be assessed simultaneously as well as $^{99m}$Tc-MIBI tumor uptake. Additional information on blood flow may be useful in some patients. For example, in Patient 8 with chondrosarcoma, only radionuclide angiography detected the lesion, and in Patient 5 with chondrosarcoma, both tracers showed faint uptake. However, radionuclide angiography showed an obviously hypervascular lesion, suggesting a malignant tumor. As shown in Figure 1, a significant correlation was observed between perfusion index and $^{99m}$Tc-MIBI uptake ratio although it was not a rigid correlation, suggesting that perfusion was not the sole determinant of tracer uptake.

In the evaluation of tumor response to chemotherapy, several modalities are used, including CT, MRI, angiography and radionuclide imaging. Although tumor size can be evaluated well by CT and MRI, estimation of residual tumor cell viability is somewhat difficult. In radionuclide imaging, Ramanna et al. (*16*) reported that $^{201}$Tl was superior to gallium and bone

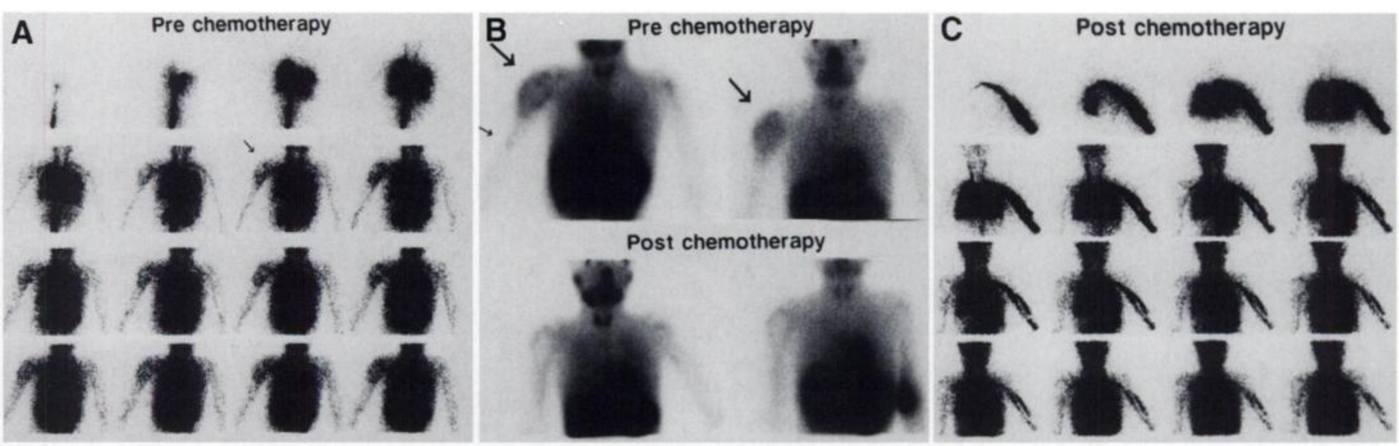


**FIGURE 4.** An 8-yr-old boy with osteosarcoma in the right proximal humerus (Patient 2). (A) Radionuclide angiography with $^{99m}$Tc-MIBI demonstrates increased perfusion of the tumor (arrow). (B) Prechemotherapeutic $^{99m}$Tc-MIBI (left upper) and $^{201}$Tl (right upper) accumulated in the lesion (large arrows), but only $^{99m}$Tc-MIBI scintigraphy discloses bone marrow extension to the humeral shaft (small arrow). After chemotherapy, both tracers show (B) markedly decreased lesion uptake and (C) perfusion. Complete tumor necrosis was verified after resection of the tumor.

scintigraphy, and Caner et al. (*17*) showed that $^{99m}$Tc-MIBI was superior to bone scintigraphy in the assessment of residual tumor viability. In this study, both $^{201}$Tl and $^{99m}$Tc-MIBI uptake ratios could evaluate tumor response to chemotherapy precisely and equally. In addition, radionuclide angiography with $^{99m}$Tc-MIBI might provide more objective information about tumor blood flow by quantification, whereas quantification of blood flow is difficult in conventional angiography with contrast media. In this study, the percent change in the perfusion index overestimated tumor response to chemotherapy in two patients with pathological nonresponse, although in both patients (Patients 12 and 23), postchemotherapeutic perfusion indices were still high (1.93 and 1.79), suggesting presence of hyperperfused residual tumor. Consequently, we believe that $^{99m}$Tc-MIBI imaging deserves to be considered one of the best methods for evaluating tumor response to chemotherapy.

When the lesion is located in the pelvic or abdominal area, $^{99m}$Tc-MIBI uptake might be significantly affected by bladder or gastrointestinal uptake. In these areas, $^{201}$Tl may be favorable because of the lower activity of the abdominal and pelvic organs. In case of disuse atrophy of the extremities due to pain or other factors, careful interpretation of uptake ratio and perfusion index are needed because muscle tracer uptake of both extremities may differ significantly and may affect these quantitative data. As shown in Figure 5, both original images and quantitative data should be always interpreted simultaneously because the uptake ratio affected significantly by the background activity in some patients.

## CONCLUSION

This study revealed that $^{99m}$Tc-MIBI has similar potential compared with $^{201}$Tl for detecting bone and soft-tissue lesions, but both tracers could not delineate benign from malignant lesions. Due to the high dose of $^{99m}$Tc-MIBI administered, the degree of blood flow can be evaluated by radionuclide angiography, which is difficult in $^{201}$Tl scintigraphy. In addition, $^{99m}$Tc-MIBI scintigraphy accurately assessed tumor response to chemotherapy as did $^{201}$Tl. Technetium-99m-MIBI scintigraphy is a promising method for evaluating bone and soft-tissue lesions, including detection and therapeutic response.

## REFERENCES


1. Hisada K, Tonami N, Miyamae T, et al. Clinical evaluation of tumor imaging with thallium-201 chloride. *Radiology* 1978;129:497–500.
2. Ancri D, Basset JY, Lonchampt MF, Etavard C. Diagnosis of cerebral lesions by thallium-201. *Radiology* 1978;128:417–422.
3. Tonami N, Shuke N, Yokoyama K, et al. Thallium-201 single-photon emission computed tomography in the evaluation of suspected lung cancer. *J Nucl Med* 1989;30:997–1004.
4. Charkes ND, Vitti RA, Brooks K. Thallium-201 SPECT increases detectability of thyroid cancer metastases. *J Nucl Med* 1990;31:147–153.
5. Waxman AD, Ramanna L, Memsic LD, et al. Thallium scintigraphy in the evaluation of mass abnormalities of the breast. *J Nucl Med* 1993;34:18–23.
6. Howman-Giles R, Uren RF, Shaw PJ. Thallium-201 scintigraphy in pediatric soft-tissue tumors. *J Nucl Med* 1995;36:1372–1376.
7. McCall D, Zimmer LJ, Katz AM. Kinetics of thallium exchange in cultured rat myocardial cells. *Circ Res* 1985;56:370–376.
8. Aktolun C, Bayhan H, Kir M. Clinical experience with Tc-99m-MIBI imaging in patients with malignant tumors. Preliminary results and comparison with Tl-201. *Clin Nucl Med* 1992;17:171–176.
9. Campeau RJ, Kronemer KA, Sutherland CM. Concordant uptake of Tc-99m sestamibi and Tl-201 in unsuspected breast tumor. *Clin Nucl Med* 1992;17:936–937.
10. O'Tuama LA, Treves ST, Larar JN, et al. Thallium-201 versus technetium-99m-MIBI SPECT in evaluation of childhood brain tumors: a within-subject comparison. *J Nucl Med* 1993;34:1045–1051.
11. Balon HR, Fink BD, Stoffer SS. Technetium-99m-sestamibi uptake by recurrent Hurthle cell carcinoma of the thyroid. *J Nucl Med* 1992;33:1393–1395.
12. Bom HS, Kim JY, Kim YC, Choi IS, Park KO. Technetium-99m-MIBI uptake in simultaneous thyroid and lung cancers. *Clin Nucl Med* 1994;19:604–606.
13. Scott AM, Kostakoglu L, O'Brien JP, et al. Comparison of technetium-99m-MIBI and thallium-201-chloride uptake in primary thyroid lymphoma. *J Nucl Med* 1992;33:1396–1398.
14. Desai SP, Yuille DL. Visualization of a recurrent carcinoid tumor and an occult distant metastasis by technetium-99m-sestamibi. *J Nucl Med* 1993;34:1748–1751.
15. Maublant JC, Zhang Z, Rapp M, et al. In vitro uptake of technetium-99m-teboroxime in carcinoma cell lines and normal cells: comparison with technetium-99m-sestamibi and thallium-201. *J Nucl Med* 1993;34:1949–1952.
16. Ramanna L, Waxman A, Binney G, et al. Thallium-201 scintigraphy in bone sarcoma: comparison with gallium-67 and technetium-MDP in the evaluation of chemotherapeutic response. *J Nucl Med* 1990;31:567–572.
17. Caner B, Kitapcl M, Unlu M, et al. Technetium-99m-MIBI uptake in benign and malignant bone lesions: a comparative study with technetium-99m-MDP. *J Nucl Med* 1992;33:319–24.
18. Carvalho PA, Chiu ML, Kronauge JF, et al. Subcellular distribution and analysis of technetium-99m-MIBI in isolated perfused rat hearts. *J Nucl Med* 1992;33:1516–1522.
19. Piwnica WD, Kronauge JF, Chiu ML. Uptake and retention of hexakis (2-methoxyisobutyl isonitrile) technetium(I) in cultured chick myocardial cells. Mitochondrial and plasma membrane potential dependence. *Circulation* 1990;82:1826–1838.
20. Beanlands RS, Dawood F, Wen WH, et al. Are the kinetics of technetium-99m methoxyisobutyl isonitrile affected by cell metabolism and viability? *Circulation* 1990;82:1802–1814.
21. Delmon-Moigeeon LI, Piwnica-Worms D, Van den Abbeele AD, Holman BL, Davison A, Jones AG. Uptake of the cation hexakis(2-methoxyisobutylisonitrile)-technetium-99m by human carcinoma cell lines in vitro. *Cancer Res* 1990;50:2198–2202.
22. Maublant JC, Zhang Z, Rapp M, Ollier M, Michelot J, Veyre A. In vitro uptake of technetium-99m-teboroxime in carcinoma cell lines and normal cells: comparison with technetium-99m-sestamibi and thallium-201. *J Nucl Med* 1993;34:1949–1952.
23. Piwnica-Worms D, Chiu ML, Budding M, Kronauge JF, Kramer RA, Croop JM. Functional imaging of multidrug-resistant p-glycoprotein with an organotechnetium complex. *Cancer Res* 1993;53:977–984.
24. Rao VV, Chiu-ML, Kronauge JF, Piwnica-Worms D. Expression of recombinant human multidrug resistance P-glycoprotein in insect cells confers decreased accumulation of technetium-99m-sestamibi. *J Nucl Med* 1994;35:510–515.
25. Cordobes MD, Starzec A, Delmon-Moingeon L, et al. Technetium-99m-sestamibi uptake by human benign and malignant breast tumor cells: correlation with mdr gene expression. *J Nucl Med* 1996;37:286–289.
26. Sehweil AM, McKillop JH, Milroy R, Wilson R, Abdel-Dayem HM, Omar YT. Mechanism of 201Tl uptake in tumors. *Eur J Nucl Med* 1989;15:376–379.
27. Caluser C, Macapinlac H, Healey J, et al. The relationship between thallium uptake, blood flow, and blood-pool activity in bone and soft-tissue tumors. *Clin Nucl Med* 1992;17:565–572.